Dynamic Compartmentalization of Bacteria: Accurate Division in *E. Coli*

Martin Howard,[1,*] Andrew D. Rutenberg,[2] and Simon de Vet[2]

[1]*Department of Physics, Simon Fraser University, Burnaby, British Columbia, Canada V5A 1S6*
[2]*Department of Physics, Dalhousie University, Halifax, Nova Scotia, Canada B3H 3J5*

(Received 14 July 2001; published 10 December 2001)

Positioning of the midcell division plane within the bacterium *E. coli* is controlled by the *min* system of proteins: MinC, MinD, and MinE. These proteins *coherently* oscillate from end to end of the bacterium. We present a reaction-diffusion model describing the diffusion of *min* proteins along the bacterium and their transfer between the cytoplasmic membrane and cytoplasm. Our model spontaneously generates protein oscillations in good agreement with experiments. We explore the oscillation stability, frequency, and wavelength as a function of protein concentration and bacterial length.

DOI: 10.1103/PhysRevLett.87.278102 PACS numbers: 87.17.Ee, 87.16.Ac, 82.39.Rt

The subcellular spatial and temporal organization of bacterial proteins is largely unknown. Already, the spatial distribution of proteins on the cytoplasmic membrane of bacteria are known to be important for chemotaxis [1] and for DNA replication [2]. Improving our understanding of how this supramolecular organization of proteins affects bacterial function represents a considerable experimental and theoretical challenge. In contrast to nucleated eukaryotic cells, no large organelles are present in the bacterial interior (cytoplasm), and no active transport mechanisms such as molecular motors are known to function there. However, recent video microscopy of fluorescently labeled proteins involved in the regulation of *E. coli* division have uncovered coherent and stable spatial and temporal *oscillations* in three proteins: MinC, MinD, and MinE [3–8]. The proteins oscillate from end to end of the bacterium, and move between the cytoplasmic membrane and the cytoplasm. These *min* proteins select the site for the next bacterial division [9,10]. Despite a wealth of phenomenological detail, no quantitative models have been developed of how the *min* proteins organize into oscillating structures. Understanding the self-organized patterns involved in bacterial division processes can give us insight into how a bacterium can dynamically compartmentalize itself.

We focus on *E. coli*, a commonly studied rod shaped bacterium, approximately 2–6 μm in length and around 1–1.5 μm in diameter. Each *E. coli* divides roughly every hour, depending on the conditions — first replicating its DNA then dividing in half to form two viable daughter cells. The MinCDE oscillations are known to persist even when protein synthesis is suppressed [3], and DNA replication and septation occur even without the *min* proteins. Hence, the *min* system can be studied independently of the other division processes. Efficient division requires many processes, including DNA replication, MinCDE oscillations, and the actual septation process. Septation initiates with a contractile polymeric "Z-ring" of a tubulin-homologue FtsZ that forms just underneath the cytoplasmic membrane. The FtsZ septation rings largely avoid guillotining the DNA-containing nucleoids independently of the *min* system [11]. This "nucleoid occlusion" serves as a complementary control mechanism for accurate cell division. The role of the *min* system appears to be to restrict the Z-ring to midcell. This reduces the production of inviable nucleoid-free minicells which occur when the cell divides too close to the cell poles. If the *min* system is genetically knocked out, 40% of the divisions lead to inviable minicells [9]—a sizable drain on bacterial resources.

The study of deletion mutants has made the phenomenological roles of the individual *min* proteins clear. MinC associated to the cytoplasmic membrane locally inhibits assembly of the contractile Z-ring, but remains cytoplasmic and largely inactive in the absence of MinD [5]. MinD binds MinC and recruits it to the cytoplasmic membrane [5,12]. MinE drives MinD away from the bacterial midplane, and, hence, allows a contractile ring to form only there. Without MinE, the membrane-bound MinC/MinD block Z-ring formation everywhere, inhibiting division, and resulting in the formation of long filamentous cells [4,6]. Without MinC, Z-ring formation cannot be inhibited anywhere and inviable minicells are produced. Without MinD, neither MinC nor MinE are recruited to the cytoplasmic membrane and so have a reduced effect.

With normal levels of MinC, MinD, and MinE, a remarkable oscillatory dynamics is seen [3–8]. First, the MinC/MinD accumulate at one end of the bacterium on the cytoplasmic membrane. Then MinE forms a band at midcell which sweeps towards the cell pole occupied by the MinC/MinD, ejecting the MinC/MinD into the cytoplasm as it goes. The ejected MinC/MinD then rebinds at the other end of the bacterium. When the MinE band reaches the cell pole, it disassociates and reforms at midcell. The entire process then repeats towards the opposite cell pole. The oscillation period is approximately 1–2 min, so many oscillations occur between each bacterial division. The dynamics minimizes the MinC/MinD concentration at midcell, thereby allowing the Z-ring and the subsequent division septum to form there.

Until recently [8], qualitative models of the *min* system involved unidentified midcell topological markers (see, e.g., [13]). This Letter puts forward the first quantitative

self-organized model that describes much of the intricate phenomenology of accurate division site placement in *E. coli*, and does so using *only* the diffusive motion and interactions of the *min* proteins. The essence of our approach is to describe the MinCDE dynamics by a set of coupled reaction-diffusion equations. Experimental results indicate that the oscillatory protein dynamics is unaffected if new protein synthesis is blocked [3]. Accordingly, we employ a model that conserves the total number of each protein type. Strikingly, this model possesses a linear Turing-like (Hopf) instability [14,15] despite the absence of mechanisms such as internal reactant production or external feed that have normally been required to model Turing patterns [16]. [Of course energy input in the form of adenosine triphosphate (ATP) is required to sustain the oscillations within a bacterium.] As we will see, the resulting protein oscillations mark the midcell with a minimum of the time-averaged concentration of MinC/MinD and with a corresponding maximum of MinE.

Our starting point is a set of four coupled reaction-diffusion equations describing, respectively, the densities of MinD on the cytoplasmic membrane (ρ_d), MinD in the cytoplasm (ρ_D), MinE on the cytoplasmic membrane (ρ_e), and MinE in the cytoplasm (ρ_E):

$$\frac{\partial \rho_D}{\partial t} = D_D \frac{\partial^2 \rho_D}{\partial x^2} - \frac{\sigma_1 \rho_D}{1 + \sigma_1' \rho_e} + \sigma_2 \rho_e \rho_d , \quad (1)$$

$$\frac{\partial \rho_d}{\partial t} = \frac{\sigma_1 \rho_D}{1 + \sigma_1' \rho_e} - \sigma_2 \rho_e \rho_d , \quad (2)$$

$$\frac{\partial \rho_E}{\partial t} = D_E \frac{\partial^2 \rho_E}{\partial x^2} - \sigma_3 \rho_D \rho_E + \frac{\sigma_4 \rho_e}{1 + \sigma_4' \rho_D} , \quad (3)$$

$$\frac{\partial \rho_e}{\partial t} = \sigma_3 \rho_D \rho_E - \frac{\sigma_4 \rho_e}{1 + \sigma_4' \rho_D} . \quad (4)$$

Following the observation in Refs. [4,5] that the MinC dynamics simply follows that of the MinD, we do not model the MinC field explicitly. We consider the variation of density along the long bacterial axis, tracking the local rates of change of the densities stemming from diffusion and from transfer between the cytoplasmic membrane and the cytoplasm. Zero flux "closed" boundary conditions are imposed at both ends of the bacterium. The total amount of MinD and MinE, obtained by integrating $\rho_d + \rho_D$ and $\rho_e + \rho_E$ over the length of the bacterium, is explicitly conserved by our dynamics.

By reducing the *min* protein dynamics to a set of deterministic $1d$ rate equations, we neglect fluctuation effects. Given that the number of *min* molecules in each cell is rather small (around 3000 for MinD [17] and 170 for MinE [18]), these fluctuations could be important. While some fluctuation effects are evident experimentally, such as an occasional midcycle reversal of the direction of MinE band propagation [8], on the whole bacterial oscillations appear to be amazingly regular [5]. Our continuum coarse-grained approach captures the essence of the protein dynamics and explains the self-organized aspects of the MinCDE oscillations.

In the first reaction terms in Eqs. (1) and (2), σ_1 describes the spontaneous association of MinD to the cytoplasmic membrane [6]. MinD is required to recruit MinE to the cytoplasmic membrane, but it is an open question whether it is cytoplasmic MinD or membrane-bound MinD that is primarily active. A cytoplasmic interaction between MinD and MinE has been observed in Ref. [12], and we are currently able to obtain the MinCDE oscillations only by allowing cytoplasmic MinD to recruit cytoplasmic MinE to the membrane, via σ_3 in Eqs. (3) and (4). Once on the membrane, MinE drives MinD into the cytoplasm. We represent this with σ_2 in the second reaction terms in Eqs. (1) and (2). Finally, MinE will spontaneously disassociate from the membrane, corresponding to σ_4 in the second reaction terms in Eqs. (3) and (4). We have not included spontaneous MinD disassociation or spontaneous MinE association terms, since experimentally MinE dominates the MinD disassociation and MinD dominates the MinE association.

Many other reaction terms are possible; however, we include only the simplest possible "renormalizations" of the basic recruitment and release terms, σ_1' and σ_4'. Effectively, σ_1' corresponds to membrane-bound MinE suppressing the recruitment of MinD from the cytoplasm, and σ_4' corresponds to cytoplasmic MinD suppressing the release of membrane-bound MinE. We have also set the diffusion constants for the membrane-bound MinD and MinE to zero. Our results are not qualitatively changed by using nonzero values, provided the membrane diffusion constants remain much less than their bulk counterparts.

For our simulations we discretized space and time with spacings of $dx = 8 \times 10^{-3}$ μm and $dt = 1 \times 10^{-5}$ s. We have checked that our results are unchanged with smaller dx and dt. Densities are measured in molecules per micron, and, unless otherwise stated, we use average densities of 1500 μm^{-1} for MinD [17] and 85 μm^{-1} for MinE [18]. The numerical values of our other parameters have not been experimentally determined for the *min* proteins. We choose cytoplasmic diffusion constants slightly less than the value 2.5 $\mu\text{m}^2\,s^{-1}$ directly measured for a maltose binding protein [19] in the *E. coli* cytoplasm. Unless otherwise mentioned, we use a length of 2 μm and the following values for the parameters in Eqs. (1)–(4): $D_D = 0.28$ $\mu\text{m}^2/\text{s}$, $D_E = 0.6$ $\mu\text{m}^2/\text{s}$, $\sigma_1 = 20$ s^{-1}, $\sigma_1' = 0.028$ μm, $\sigma_2 = 0.0063$ $\mu\text{m/s}$, $\sigma_3 = 0.04$ $\mu\text{m/s}$, $\sigma_4 = 0.8$ s^{-1}, and $\sigma_4' = 0.027$ μm.

We have analyzed the linear stability of Eqs. (1)–(4) [15]. Testing solutions of the form $e^{\lambda t + iqx}$ with the above parameter values, we find a complex $\lambda(q)$ with a positive real part that is maximized for $q \approx 1.5$ μm^{-1}, where $\lambda_{\text{max}} = 0.010 \pm 0.043i$. This indicates the presence of a maximally linearly unstable oscillating mode with a wavelength of 4.2 μm and a period of 145 s. This finding is confirmed by a direct numerical stability analysis of our

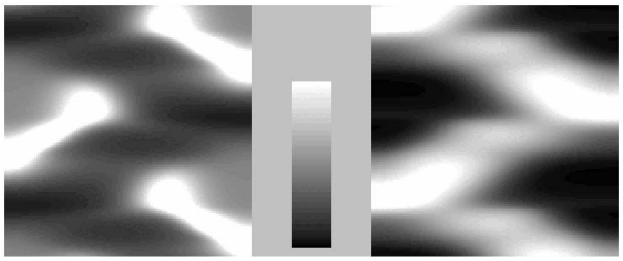

FIG. 1. Space-time plots of the total MinD (left) and MinE (right) densities. The grey scale runs from 0.0 to 2.0 times the average density of MinD or MinE, respectively. The MinD depletion from midcell and the MinE enhancement at midcell are immediately evident. Time increases from top to bottom, and the pattern repeats indefinitely as time increases. The grey-scale reference bar spans 100 s. The horizontal scale spans the bacterial length (2 μm).

model (not shown). The physical origin of this instability lies in the disparity between the membrane and cytoplasmic diffusion rates, and also in the slower rate at which MinE disassociates from the membrane. This ensures that the MinE dynamics lags that of the MinD, setting up the oscillating patterns. The existence of the linear instability in Eqs. (1)–(4) is crucial, since it means that the oscillating pattern will spontaneously generate itself from a variety of initial conditions — including nearly homogeneous ones. In our simulations, we used random initial conditions, although identical patterns were also observed with asymmetric initial distributions of MinD and MinE. The eventual oscillating state is stabilized by the nonlinearities in Eqs. (1)–(4). At the midcell, this oscillating pattern has a minimum of the time-averaged MinD concentration — an essential feature of division regulation — and a maximum of the time-averaged MinE concentratio.

Space-time plots of the MinD and MinE concentrations for a cell length of 2 μm are shown in Fig. 1. In excellent agreement with the experimental results, the MinE spontaneously forms a single band at midcell which then sweeps towards a cell pole, displacing the MinD, which then reforms at the opposite pole. Once the MinE band reaches the cell pole it disappears into the cytoplasm, only to reform at midcell where the process repeats, but in the other half of the cell. These patterns are stable over at least 10^9 iterations (10^4 s) — long enough for the *min* system to regulate cell division throughout the division cycle of the cell. In Fig. 2, we plot the time-averaged MinD and MinE densities as a function of position. MinD shows a pronounced dip in concentration close to midcell, which allows for the removal of division inhibition at midcell. This is in qualitative agreement with the experimental data of Ref. [8]. MinE peaks at midcell, with a minimum at the cell extremities.

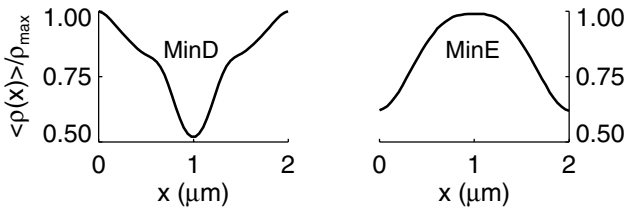

FIG. 2. The time-average MinD (left) and MinE (right) densities, $\langle \rho(x) \rangle / \rho_{\max}$, relative to their respective time-average maxima, as a function of position x (in μm) along the bacterium.

We also investigated longer filamentous bacteria and found a multiple MinE band structure (not shown). Multiple MinE bands always combined into a single MinE band in cell lengths shorter than the natural wavelength indicated by linear stability analysis.

The oscillation period as a function of the average MinD concentration is shown in Fig. 3 (left). We find a linear relationship indicated by the best-fit line, where the period approximately doubles as the MinD concentration is quadrupled. A linear relationship has also been suggested experimentally [3]. The period of oscillation as a function of cell length is shown in Fig. 3 (right). Below lengths of 1.2 μm the bacterium does not sustain oscillating patterns. For lengths above this minimum, the oscillation patterns are stable and the period increases with length — as observed experimentally [7]. The periods measured from our numerics for cell lengths of 2 μm are around 100 s, in good agreement with experiments, where periods from 30–120 s have been found [3]. A single MinE band state is stable over a wide range of lengths for a given density of *min* proteins. This provides strong evidence that the *min* system is capable of regulating accurate cell division over normally occurring cell lengths as the cell grows between division events. At longer lengths of around 6 μm, we observe long-lived metastable states with two MinE bands. These multiple bands can survive for a thousand seconds or more before decaying into a single band. At still longer lengths the two band state appears stable; this occurs around 8.4 μm — twice the dominant wavelength given by the linear stability analysis. This explains why the characteristic wavelength of linear stability analysis is rather longer than a normal *E. Coli* bacterium — if the length scale were smaller, then multiple MinE bands might

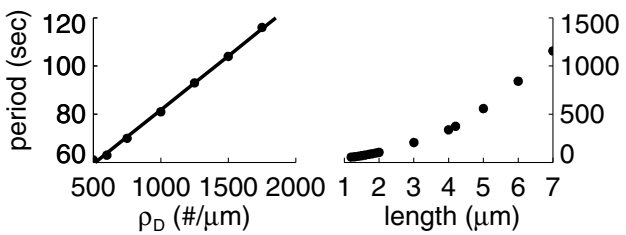

FIG. 3. Left: Plot of the period of oscillation (in seconds) against MinD density (in μm^{-1}), at fixed average MinE concentration of 85 μm^{-1}. The solid line is a linear best fit. Right: Plot of oscillation period against cell length, for fixed MinD and MinE concentrations. Below bacterial lengths of 1.2 μm, oscillation is not observed.

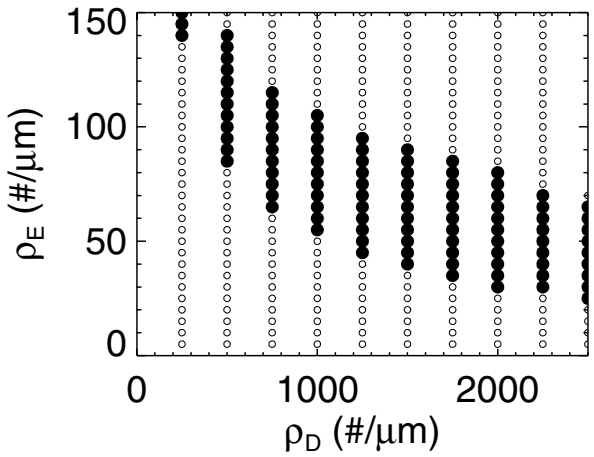

FIG. 4. Filled circles indicate regions of linear instability vs the density of MinD and MinE, where small inhomogeneities grew into a periodically oscillating pattern. Open circles indicate regions of linear stability where small inhomogeneities decay into a uniform and static pattern.

occur in bacteria of normal lengths and proper division regulation would be inhibited.

If the MinD concentration is increased or decreased beyond the limits shown in Fig. 3 (left), then the oscillation amplitude decays, and a uniform steady state results. The stability is mapped out in Fig. 4, as a function of protein concentration. This is consistent with experiment, where overexpression of MinD suppresses division [9]. Although varying the MinE concentration does affect the region of oscillatory instability (as shown in Fig. 4), it did not have a significant effect on the oscillation period. This appears somewhat contrary to the results of Ref. [3], possibly due to the absence of MinE dimerization in our model [20].

In conclusion, we have introduced a particle-conserving reaction-diffusion model that self-organizes to form a key regulatory mechanism for accurate midcell division site selection in *E. coli*. The model qualitatively agrees with many of the features found in experiments, and, in particular, naturally accounts for the oscillatory patterns of the *min* proteins. Already, our model leads us to make a number of striking predictions: We require that cytoplasmic MinD recruits MinE to the membrane; we require that the membrane-associated diffusion constants for MinD and MinE are very much less than their corresponding values in the cytoplasm; and we have mapped out the shape of the oscillation regime as a function of average MinD and MinE concentration.

Experimental characterization of reaction rates and diffusion constants do not yet severely constrain our model. Accurate experimental measurements of oscillation periods and wavelengths as a function of concentrations of MinD and MinE will provide a stringent test. There is also considerable scope for extending our results. In subsequent studies, we will explore a bulk $3d$ system with discrete particle dynamics and microscopic interactions between individual protein molecules. This will allow us to explicitly consider the influence of fluctuations due to discrete particles, the role of ATPase activity of MinD [17], and the effects of MinE dimerization [20].

This work was supported financially by NSERC Canada. We would like to thank Russell Bishop for encouragement and useful comments and Michael Greenwood for his development of imaging software.

*Current address: Instituut-Lorentz, Leiden University, P.O. Box 9506, 2300 RA Leiden, The Netherlands.

[1] N. Maki *et al.,* J. Bacteriol. **182**, 4337 (2000).
[2] K. P. Lemon and A. D. Grossman, Science **282**, 1516 (1998).
[3] D. M. Raskin and P. A. J. de Boer, Proc. Natl. Acad. Sci. U.S.A. **96**, 4971 (1999).
[4] D. M. Raskin and P. A. J. de Boer, J. Bacteriol. **181**, 6419 (1999).
[5] Z. Hu and J. Lutkenhaus, Mol. Microbiol. **34**, 82 (1999).
[6] S. L. Rowland *et al.,* J. Bacteriol. **182**, 613 (2000).
[7] X. Fu *et al.,* Proc. Natl. Acad. Sci. U.S.A. **98**, 980 (2001).
[8] C. A. Hale, H. Meinhardt, and P. A. J. de Boer, EMBO J. **20**, 1563 (2001).
[9] P. A. J. de Boer, R. E. Crossley, and L. I. Rothfield, Cell **56**, 641 (1989).
[10] L. Rothfield, S. Justice, and J. García-Lara, Annu. Rev. Genet. **33**, 423 (1999).
[11] X.-C. Yu and W. Margolin, Mol. Microbiol. **32**, 315 (1999).
[12] J. Huang, C. Cao, and J. Lutkenhaus, J. Bacteriol. **178**, 5080 (1996).
[13] L. I. Rothfield and C.-R. Zhao, Cell **84**, 183 (1996).
[14] M. C. Cross and P. C. Hohenberg, Rev. Mod. Phys. **65**, 851 (1993).
[15] J. D. Murray, *Mathematical Biology* (Springer-Verlag, Berlin, 1993), 2nd ed.
[16] H. Meinhardt, *Models of Biological Pattern Formation* (Academic Press, London, 1982).
[17] P. A. J. de Boer *et al.,* EMBO J. **10**, 4371 (1991).
[18] C.-R. Zhao, P. A. J. de Boer, and L. I. Rothfield, Proc. Natl. Acad. Sci. U.S.A. **92**, 4313 (1995).
[19] M. B. Elowitz *et al.,* J. Bacteriol. **181**, 197 (1999).
[20] G. F. King *et al.,* Mol. Microbiol. **31**, 1161 (1999).